Research Article Vol. 42, No. 5 / May 2025 / Journal of the Optical Society of America A B167

Journal of the Optical Society of America A
OPTICS, IMAGE SCIENCE, AND VISION

Effect of stimulus size on chromatic discrimination

M. V. Danilova[1,2,*] and J. D. Mollon[2]

[1]Kharkevich Institute for Information Transmission Problems, Moscow, Russia
[2]Department of Psychology, University of Cambridge, Cambridge, UK
*mvd1000@cam.ac.uk

Received 21 October 2024; revised 21 December 2024; accepted 22 December 2024; posted 24 December 2024; published 4 February 2025

In psychophysical experiments, discrimination thresholds were measured in different directions around points in the MacLeod–Boynton chromaticity diagram, while the eye was maintained in a state of constant adaptation to a metamer of D65. A spatial forced-choice procedure was used: a brief (150 ms) disk divided into four sectors was presented, and the observers' task was to detect the sector that differed from the other three. The diameter of the test disk varied from 32 min to 2.4° of visual angle. Sensitivity was probed at several different referent positions in the chromaticity diagram, including the adapting chromaticity. The data for each referent were fitted with ellipses. In the case of the largest test size (2.4° diameter), ellipses were predominantly oriented so that their longer axis was aligned with the line connecting the center of the ellipse to the chromaticity of D65 (the adaptation point). Along such radial lines, colorimetric purity varies, and the orientation of the ellipses reflects reduced sensitivity to saturation differences compared to hue differences. With decreasing test size, the ellipses change their orientation so that their longer axis is rotated toward a tritan direction, and the detection of changes in chromaticity depends primarily on the activity of long- and middle-wave cones. However, these general principles must be modified in several ways according to the region of the chromaticity diagram that is being probed.

https://doi.org/10.1364/JOSAA.545292

1. INTRODUCTION

Several classical studies suggested that chromatic discrimination deteriorates as the sizes of the stimuli are reduced. This was the case for measurements along the spectrum locus, i.e., wavelength discrimination (e.g., [1]), and for measurements in the interior of chromaticity space (e.g., [2,3–5]). However, almost all these studies face an interesting problem: the size of the targets is likely to be confounded with the degree to which the observer is adapted to the local region of chromaticity space in which the targets lie.

Craik [6] classically showed that luminance discrimination is optimal close to the current adaptation level, and thresholds rise rapidly when the discriminanda differ from that level. An analogous phenomenon is found for color discrimination [7–10]. Consider the implications of this finding for the discrimination ellipses of MacAdam, described in Ref. [11] in 1942. MacAdam's measurements were made at 25 points in the CIE chromaticity diagram. Although the target fields were surrounded by a neutral white field, the observer would have become adapted—at least partially—to the region of the reference chromaticity, as he adjusted the centrally viewed comparison field. When a different reference chromaticity was being used, the observer would be in a different state of adaptation. Thus, the MacAdam ellipses cannot represent human color discrimination, as it stands at any single time; they will, for example, give far too large a value if they are used to estimate the number of discriminable colors, and it is inappropriate to use them to derive uniform color spaces.

Now, consider experiments on discrimination as a function of size. Brown [2] used matching fields of either 12 or 2 degrees of visual angle and measured discrimination by the method of average error, i.e., by the standard deviation of successive matches. The matched colors were red, green, blue, and white; the surrounding fields could be red, green, blue, white, or black. Discrimination was better in all cases for the larger fields; significantly, it was only in the case of the smaller stimuli that a surrounding field of a different color had a detrimental effect on discrimination. The best discrimination in these cases was obtained either with a dark field or with a surrounding of the same hue as the referent stimulus. We can readily suppose that a 12° field allowed the observer to become fully adapted to the chromaticity region being tested, whereas in the case of the 2° field, his state of adaptation was partly determined by the surroundings. The problem becomes even more obvious in measurements made in 1959 by MacAdam [3], who compared discrimination for fields of either 3 minutes or 4.4 degrees of arc.

In the former case, the fields to be compared were 6 min apart. A neutral surround field was present in both cases. Clearly, since eye movements were unconstrained, there would be relatively little adaptation to the color of the smaller test stimuli, and the observer's state of adaptation would be predominantly determined by the neutral field, whatever the region of chromaticity space that was being tested. In the case of the 4.4° field, by contrast, the observer would be predominantly adapted to the discriminanda themselves.

To sidestep these problems, the present experiments followed the procedure introduced by Krauskopf and Gegenfurtner [8]: the retina is held in a state of neutral adaptation, and chromatic discrimination is probed at different points in the chromaticity diagram using very brief stimuli that should themselves minimally perturb the state of adaptation. In addition, we introduced small luminance pedestals, concurrent with the test stimuli, in order to better isolate chromatic channels [12].

Discrimination ellipses were measured for several regions of the MacLeod–Boynton chromaticity diagram [13] and for three different sizes of the stimulus array. The data presented are the averages for six observers who completed all the conditions. However, for every reference chromaticity, at least 10 observers were tested; and the summary data are available in Supplement 1.

Discrimination was tested for a referent at the chromaticity of the adapting field (metameric to Illuminant D65) and for referents that lay along significant lines in the MacLeod–Boynton diagram, including the tritan line passing through D65 (i.e., a line along which only the short-wave cone signal is varying), a horizontal line along which only the relative excitation of long-wave and middle-wave cones varies, and a line that corresponds approximately to the yellow–blue axis of the color space (see Fig. 1). Since there is a particular interest in the comparison of hue discrimination and saturation discrimination [14–18], at each referent chromaticity, thresholds were explicitly measured along a line of varying colorimetric purity (i.e., a line passing radially through D65 and through the referent being measured) and along a line orthogonal to this line.

2. METHODS

A. Apparatus and Calibration

The stimuli were presented on a calibrated Mitsubishi Diamond Pro 2070 22 in. CRT monitor set at a resolution of 1024 × 768 pixels and a frame rate of 100 Hz. The monitor was controlled by a Cambridge Research Systems (CRS, UK) VSG2/3 graphics board, which allows chromaticities to be specified with a precision of 15 bits per gun. The output of each gun was obtained with a silicon photodiode (OptiCal, CRS) to linearize gamma functions. The spectral power distribution for each gun at maximal output was measured with a JETI spectroradiometer model Specbos 1201 (JETI Technische Instrumente GmbH, Jena, Germany) to generate a matrix that converted the required L-, M-, and S-cone excitations into R, G, and B voltages.

B. Stimuli

The stimuli were disks, separated into four sectors by thin lines of the same chromaticity as the neutral background (a metamer of D65): three sectors were of the same chromaticity, and one differed. The separating lines serve to make the sectors distinct from each other and to achieve optimal performance: both in the fovea and in the parafovea, small gaps improve discrimination compared to adjacent or to spatially well-separated stimuli [19,20]. The average luminance of the disk was 30% higher than that of the background, but each sector was independently and randomly jittered in L + M within ±5%, with a step of 0.2% to ensure that the observers could not base their judgments on differences in luminance between the sectors. The stimulus was presented for 150 ms. Viewing was binocular from 57 cm.

The stimuli were specified in a MacLeod–Boynton chromaticity diagram [13] constructed from the 2° cone fundamentals of DeMarco *et al*. [21]. The diagram represents a plane of equal luminance for the Judd (1951) observer, where luminance is equal to the sum of the L- and M-cone excitations. Figure 1 shows a section of the diagram, where R, G, and B represent the chromaticities of the guns of the CRT monitor, and the black dotted line indicates part of the spectrum locus. The chromaticities that can be reproduced on the screen are located within the triangle with apices R, G, and B, but luminance is limited by the maximal outputs of each gun. The diagram was scaled so that the line representing chromaticities that appear neither reddish nor greenish [22] has a slope of 135°. Throughout this paper, the orientation of the ellipses and of relevant lines in the diagram will be specified in degrees, where 0° corresponds to the right horizontal from the adaptation point.

The three diameters of the disks were 32 angular minutes, 48 angular minutes, and 2.4 angular degrees. The smaller stimuli cover the central part of the fovea, where the density of S-cones is low [23], and the largest size is slightly larger than the standard 2° stimulus. It should be noted that the area of each sector was $^1/_4$ of the area of the disk.

Discrimination thresholds were measured around 10 referent chromaticities (ellipse centers), as shown in the MacLeod–Boynton diagram [Fig. 1(a)] and in the CIE 1960 uv diagram [Fig. 1(b)]. The first referent was D65 itself (gray triangle in Fig. 1). For this referent, only hue discrimination was measured, owing to the chosen procedure. For the two referents on the vertical line through D65 in the MacLeod–Boynton diagram (downward triangles in Fig. 1), purity discrimination depends only on signals from S-cones. For the two referents on the horizontal line through D65 (diamonds in Fig. 1), purity discrimination depends only on signals from L- and M-cones. Two referents were placed on the line that runs at 135°. This line is important, as it separates the human chromaticity space into greenish hues and reddish hues [24–26]. Purity discrimination for the two stimuli along this line (circles in Fig. 1) corresponds to concurrent increases in the ratios M/(L + M) and S/(L + M), whereas these ratios are out of phase for hue discrimination. One referent was located on the line running through D65 at 45° (upward triangle in Fig. 1), where purity discrimination corresponds to in-phase changes in L/(L + M) and S/(L + M) [15]. Two referents (squares in Fig. 1) were placed on a second oblique line running at 165° between the upper left and lower right quadrants of the MacLeod–Boynton space, since in natural scenes, a high density of chromaticities fall in these quadrants [27]. The chosen locations of the referents

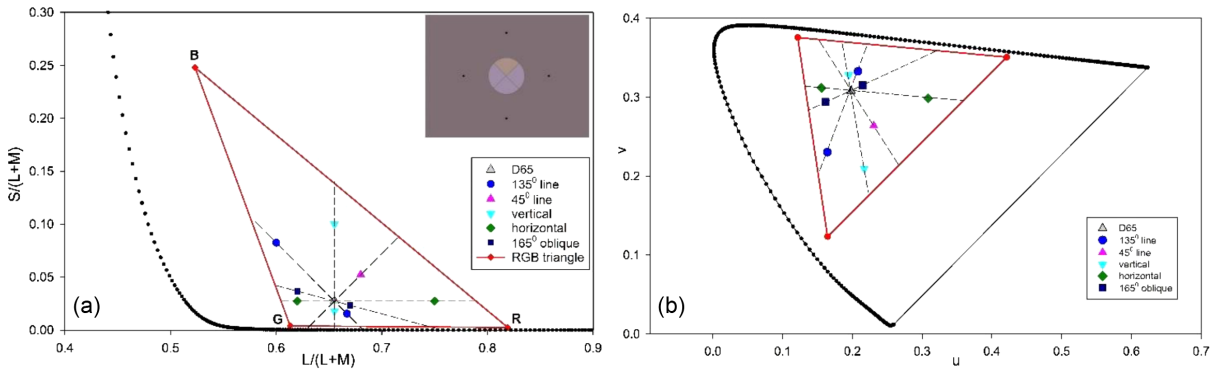

Fig. 1. (a) A section of the MacLeod–Boynton diagram showing the chromaticities of the monitor guns (R, G, and B) and locations of the referent chromaticities around which discrimination thresholds were measured. Circles represent the referents located on the line connecting unique yellow and unique blue, which passes through D65 at 135°; the upward triangle represents a referent on the line passing D65 at an angle 45°; the downward triangles represent the referents located on the vertical line through D65; the diamonds represent referents located on the line that runs horizontally through D65; and the squares represent referents located on the oblique line passing through D65. Inset: a screenshot of the central part of the screen with the stimulus. In this example, the upper sector differs from the other three: the difference between the sectors is exaggerated for illustration purposes. Four black dots around the stimulus helped observers to fixate the center of the screen. (b) Locations of the 10 referent chromaticities in the 1960 uv diagram.

along the selected lines depended on the monitor gamut and the luminance available.

C. Procedures

In separate sets of experiments, discrimination thresholds were measured for each referent point in the chromaticity diagram. The three sizes were tested in randomly interleaved sessions. The measurements for different referent chromaticities were completed on different experimental days.

Every session tested discrimination along eight lines through the referent chromaticity with angles from 0° to 157.5°, with a step of 22.5°. In a forced-choice procedure, on each presentation, the observer was asked to identify the sector that differed in chromaticity from the other three and to press the corresponding button on a response box. The referent itself was never presented; instead, the two chromaticities (discriminanda) straddled the referent point. The chromatic separation of the discriminanda was increased or decreased symmetrically along a chosen line around the referent, according to the observer's accuracy. The observers were given auditory feedback after they had responded. The staircase procedure tracked a 79.4% correct response rate on the psychometric function [28]. After three correct responses, the separation of chromaticities was reduced by 10%, and after each incorrect response it was increased by 10%. The staircase procedure was terminated after 15 reversals, the last 10 reversal points being averaged to give the threshold. This technique gives 16 values around the reference chromaticity: each pair of points along one line through the referent represents the threshold distance between two chromaticities.

D. Observers

A total of 31 observers participated in the experiments. Six observers completed all three sizes for all 10 referent chromaticities, and their data are presented in the main body of the paper. An additional 25 observers completed measurements for only a few references in the full set of 10 referent chromaticities. For each referent chromaticity, data were collected for 10–13 observers. The observers were randomly assigned to one or more of the references. The average data for all the observers are presented in Supplement 1.

All observers had normal color vision as tested with the Ishihara plates (illuminated by a Macbeth Daylight Lamp) and with the OSCAR test [29]. The study was conducted under the tenets of the Declaration of Helsinki. The experimental measurements were made in the Vision Laboratory of the Department of Psychology, University of Cambridge, and were approved by the Cambridge Psychology Research Ethics Committee.

3. RESULTS

Figures 2–7 present the results for each referent chromaticity. In each case, the 16 symbols show the thresholds along each of the eight lines that were tested for each referent chromaticity. The paired chromaticities lying on the same line passing through the referent chromaticity are those that can be discriminated by an observer at the level of 79.4% correct response rate [28], according to the 3:1 staircase procedure (see Section 2).

The shapes formed by 16 dots are close to elliptical, and therefore were fitted with ellipses using the direct least squares method of Fitzgibbon *et al*. [30].

On the basis of average results for six observers, Table 1 gives values for the longer and shorter axes of the ellipses and their orientations for three sizes of the tests. Table S1 (Supplement 1) gives the corresponding data for all the participating observers.

For all the referents, in agreement with earlier studies, larger test fields yield smaller discrimination thresholds—the distances of the dots from the referent chromaticity are the smallest. With decreasing size, the distances from the referent increase, indicating the increase in discrimination thresholds (Figs. 2–7).

However, the shape of the ellipses changes with size in different ways for different referent chromaticities. In the case of each referent, a one-way ANOVA was conducted with target size as

factor. If the normality test failed, a Kruskal–Wallis test on ranks was performed.

A. Discrimination Ellipses Centered at D65

Figure 2 shows average data and fitted ellipses for the referent located at the adapting chromaticity D65. Chromaticity discrimination around this neutral point in the color space is of special interest (e.g., [31–33]). As the size of the test increases, the fitted ellipse changes its orientation from nearly vertical to almost diagonal. A one-way repeated measurement ANOVA confirms significant changes in orientation: $F[2] = 15.72$, $p < 0.001$. The orientation of the major axis is 101.5° for the smallest size, but 147.5° for the largest size (see Table 1, ellipse 1). If the ellipse were aligned with the diagonal, its orientation would be 135°. For the group of six observers, the ellipse is not exactly aligned with this diagonal but is rotated slightly counterclockwise relative to the blue–yellow line in the scaled MacLeod–Boyton diagram. The larger group of observers shows the same pattern (see Supplement 1, Fig. S1).

The ellipses also change their shape and become more circular with an increasing test size: the ratio between the long and the short axes of the ellipse changes from 2.92 (diameter 32 min) to 2.16 (diameter 48 min) and to 1.45 (diameter 2.4°).

B. Discrimination Ellipses Centered on the Vertical Line through D65 (Running at 90° in the Diagram)

Figure 3(a) shows results for the referent lying below D65 but on the (vertical) tritan line that passes through D65. For the largest test, the ellipse takes a form close to a circle, but with a decreasing test size, the ellipses become more and more aligned

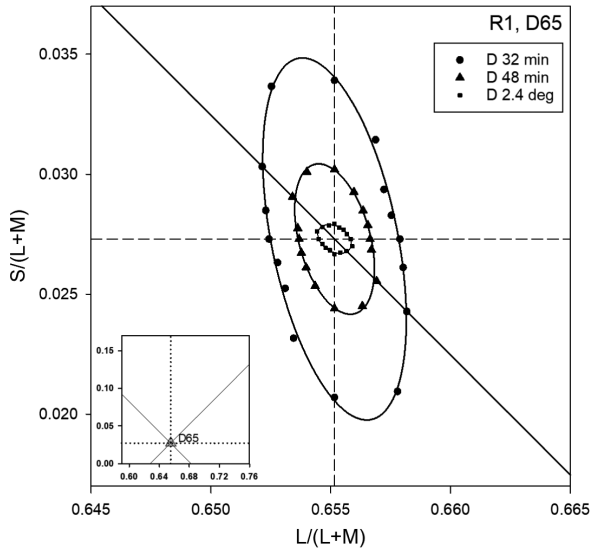

Fig. 2. Discrimination around D65, the adapting chromaticity (R1). The dashed lines correspond to the two cardinal directions of the MacLeod–Boynton diagram. The solid line has a slope of −1 (135° counterclockwise from the right horizontal) in our scaled diagram (see Section 2). The three ellipses correspond to the three sizes of test stimulus, and the data points are averages of six observers. In this and subsequent figures, the inset shows the position of the referent in the MacLeod–Boynton diagram.

with the tritan line through D65. For the smallest target, the ellipse is rotated slightly away from the tritan line (see also Table 1, ellipse 4). A Kruskal–Wallis test did not show a significant variation in the orientations of the fitted ellipses for the six observers: $H[2] = 3.19$, $p = 0.203$. However, the larger group of 12 observers shows a significant variation (see Supplement 1).

Figure 3(b) presents the results for the referent placed on the same line, but with its center above D65 at a higher value of S/(L + M). When the diameter of the test is 2.4°, the ellipse is aligned with the tritan line through D65, but when the size becomes smaller, the ellipse becomes more elongated, and its longer axis is slightly rotated counterclockwise (see Table 1, ellipse 5), as was in the case of the first ellipse along the same line [Fig. 3(a)]. A one-way ANOVA showed significant variations in the orientations of the fitted ellipses: $F[2] = 11.6$, $p < 0.001$.

C. Discrimination Ellipses Centered on the Horizontal Line through D65

Two referent points were placed on the horizontal line through D65: one has an L/(L + M) value lower than that of D65 [Fig. 4(a)], and for the second one, it is higher [Fig. 4(b)]. For these points, discrimination of saturation depends only on the excitation of the L- and M-cones. For the referent where the L/M ratio was lower than that for the adapting chromaticity, D65, the largest target yields a nearly horizontally oriented ellipse [Fig. 4(a)], but the ellipse is not exactly aligned with the horizontal axis (Table 1, Referent 4). With a decreasing test size, the ellipse rotates so that the data points for the smallest test are fitted by a nearly vertical ellipse. A Kruskal–Wallis test confirms significant changes in the orientation for these ellipses: $H[2] = 11.47$, $p = 0.003$. For the second referent point on the same line, where the L/M ratio is higher than for the adapting chromaticity D65, the largest size gives an ellipse aligned with the horizontal line [Fig. 4(b), Table 1, Referent 5]. The smaller tests give data points that are fitted with ellipses rotating toward the tritan line through the referent point, and the smallest size produces an ellipse oriented obliquely at an angle of 136.7°, which is close to the orientation of the blue–yellow line (135°) in our scaled MacLeod–Boynton diagram. This rotation is significant: $F[2] = 61.35$, $p < 0.001$.

D. Discrimination Ellipses Centered on the Blue–Yellow Line (Running at 135° in the Scaled MacLeod–Boynton Diagram)

Two referents were placed on the line passing through D65 with a slope of 135° (the blue–yellow line, see Section 2) in the scaled MacLeod–Boynton diagram. Colorimetric purity varies along this line. Figure 5 shows the results. The ellipses centered at a low L/(L + M) value change their size when the size of the test changes, but not their orientation [Fig. 5(a); see also Table 1, Referent 6]. A one-way ANOVA confirms this observation: The variation in orientation of the three fitted ellipses is not significant: $F[2] = 0.187$, $p = 0.831$. The ellipses centered at a high L/(L + M) value change both their size and their orientation [Fig. 5(b); Table 1, Referent 7]. A one-way ANOVA confirms significant differences between the orientations of the fitted ellipses for different sizes: $F[2] = 8.86$, $p = 0.003$.

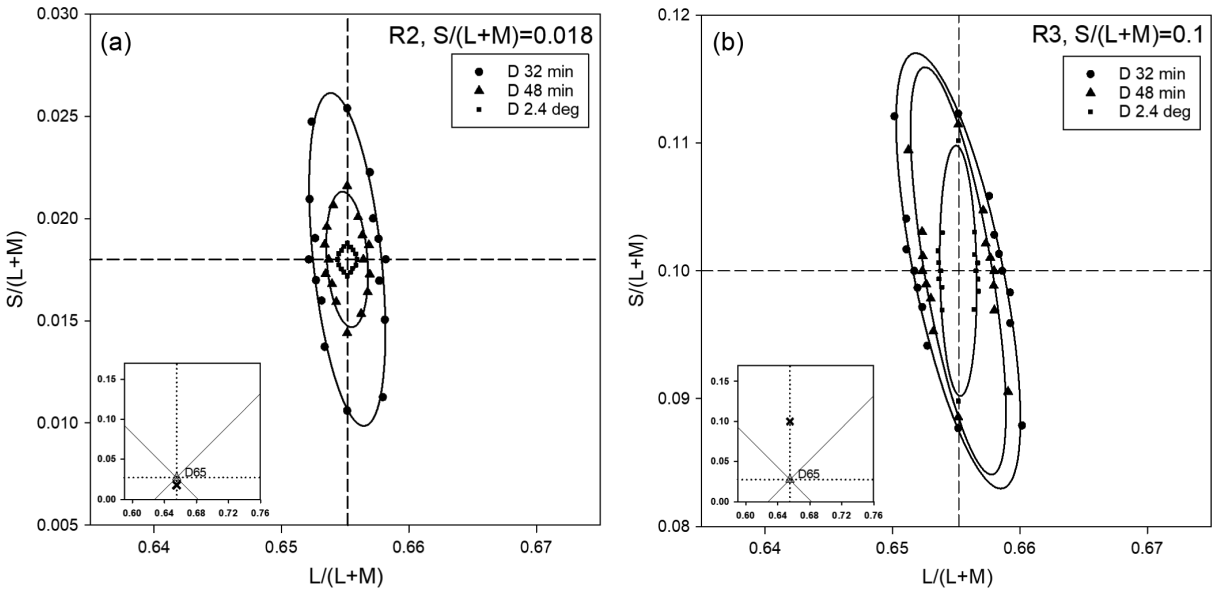

Fig. 3. (a) Results for the referent chromaticity (R2) located on the vertical line through D65 in the yellow–green section of the diagram. (b) Analogous results for the referent chromaticity (R3) located on the vertical line through D65 in the violet–pink region of the diagram.

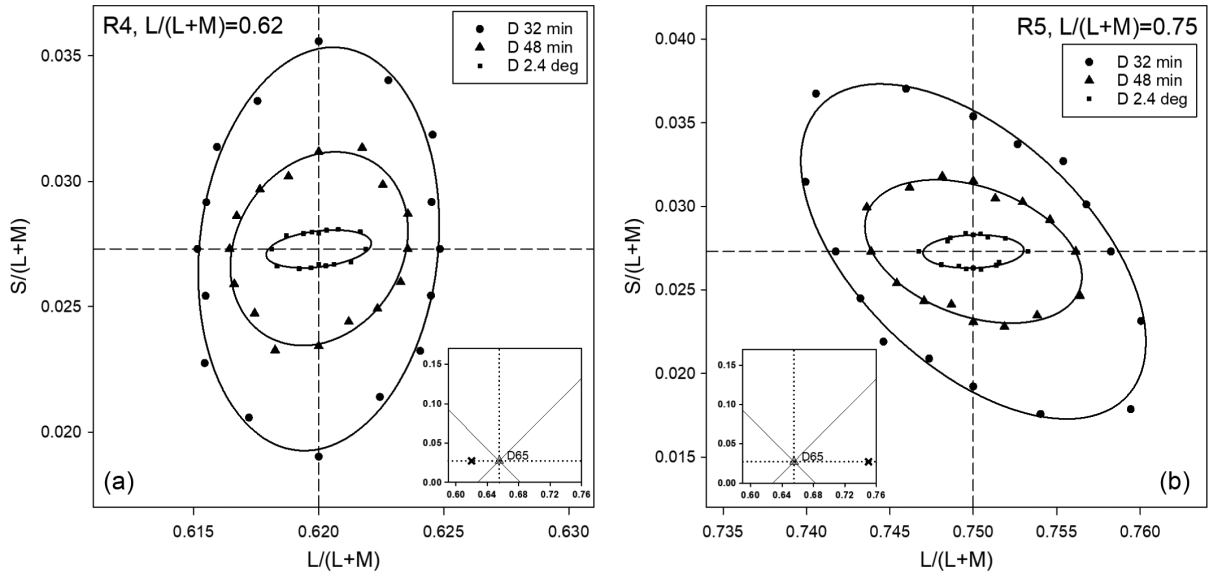

Fig. 4. (a) Results for the referent chromaticity (R4) located on the horizontal line through D65 in the bluish–greenish section of the diagram. (b) Analogous results for the referent chromaticity (R5) located on the same horizontal line, but in the reddish orange region of the MacLeod–Boynton diagram.

E. Discrimination Ellipse Centered on the Line Running at 45° through D65

Figure 6 presents the data for the referent point on the line running at an angle of 45° with both L/(L + M) and S/(L + M) coordinates higher than that of the adapting chromaticity D65. Here, perception of saturation depends on the signals of the two cardinal mechanisms added in-phase. For the largest test diameter, the fitted ellipse is not aligned with the purity line: its orientation is 72.7° instead of 45° (Fig. 6; see also Table 1, Referent 8). With a decreasing size, the fitted ellipses rotate counterclockwise, becoming almost vertical for the medium size and then tilting anticlockwise away from the tritan line. A similar counterclockwise tilt from the tritan line was already observed for the referent point placed on the horizontal line running through D65 when the referent chromaticity has L/(L + M) value higher than that of the adapting chromaticity D65 [see Fig. 5(b)]. A one-way ANOVA shows that the rotation is significant: $F[2] = 31.16, p < 0.001$.

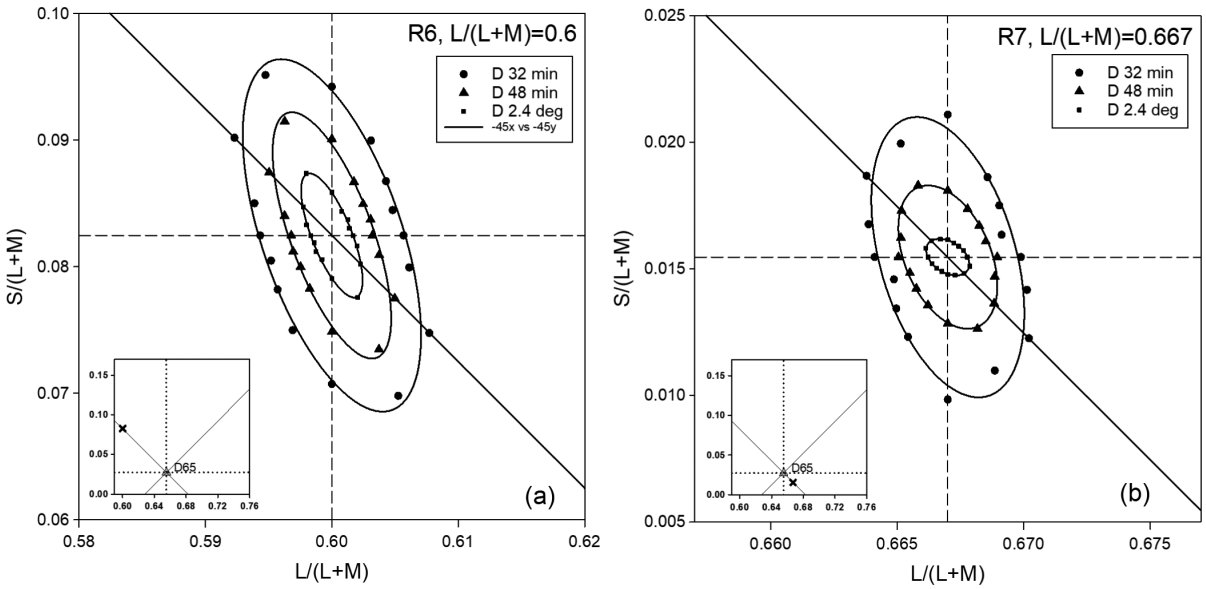

Fig. 5. (a) Results for the referent chromaticity (R6) located in the blue section of the diagram. The solid oblique line has a slope of 135°. (b) Analogous results for the referent chromaticity (R7) located in the yellow section of the diagram.

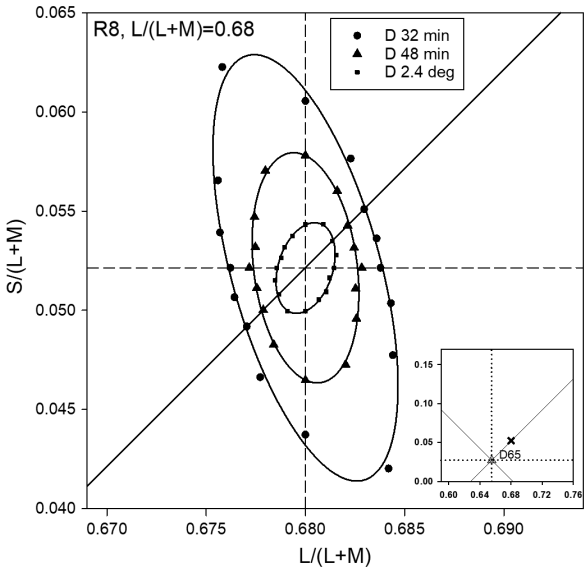

Fig. 6. Results for the referent chromaticity (R8) located on the line through D65 running at the angle +45° in the pink section of the diagram.

F. Discrimination Ellipses Centered on the Oblique Line Running at 165° through D65

Two referent chromaticities were placed on an additional oblique line through the neutral point (Fig. 7). One point has an L/(L + M) value lower than that of the adapting chromaticity D65 [Fig. 7(a)], and the second one has a higher L/(L + M) value [Fig. 7(b)].

For the largest test size, the referent point (R9) with an L/(L + M) value lower than that of D65 shows an ellipse aligned with the colorimetric purity line. This ellipse changes its form to nearly circular with decreasing size and then becomes almost vertical for the smallest size [Fig. 7(a)]. A one-way ANOVA fails to show significant changes in the orientation of the fitted ellipses: $F[2] = 3.61$, $p = 0.052$, but with the larger group of observers, this factor is significant (see Supplement 1).

In the case of the referent with an L/(L + M) value higher than that of D65, the fitted ellipse for the largest test is rotated slightly away from the purity line, toward the horizontal line: its angle is 159.8° [Fig. 7(b); see also Table 1, Referent 10]. With a decreasing size, the ellipse becomes wider and rotates toward the vertical line, continuing rotating in the same direction for the smallest size, but not actually reaching a vertical orientation [Fig. 7(b)]. A one-way ANOVA showed that the fitted ellipses differ significantly in orientation: $F[2] = 62.16$, $p < 0.001$.

4. DISCUSSION

Discrimination ellipses were measured under a constant state of adaptation at 10 locations in the scaled MacLeod–Boynton diagram and for three sizes of the test field. Figure 8 shows, in single plots, all 10 ellipses for the smallest size and for the largest size. To make the ellipses for the 2.4° targets clearly visible, they have been magnified by a factor of four (Fig. 8, right panel). For the 32 min targets (Fig. 8, left panel), the ellipses are plotted without magnification.

A. General Properties of the Discrimination Ellipses

Two general principles describe the ellipses:

(i) For large targets, the long axes of the ellipses often point away from the neutral point, i.e., they correspond—approximately—to the direction of increasing colorimetric purity (the correlate of the subjective dimension of saturation).

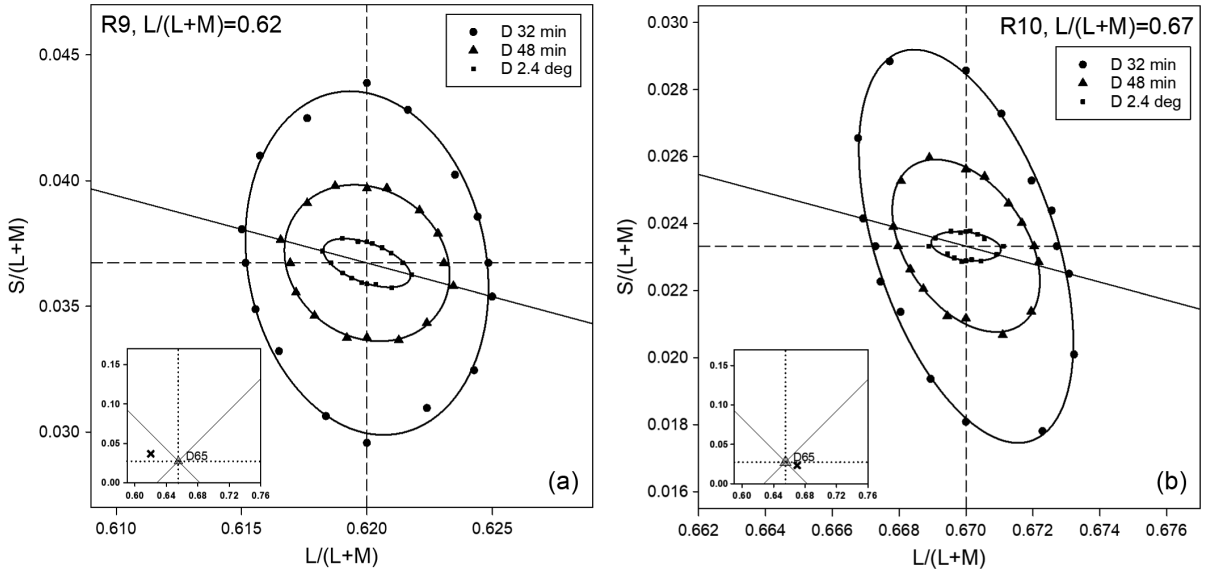

Fig. 7. (a) Results for the referent chromaticity (R9) located on a line running at 165° through D65 (solid line), in the greenish blue section of the diagram. (b) Results for the second referent chromaticity (R10) on the same line, but in the red–orange section of the chromaticity diagram.

Table 1. Parameters of the Fitted Ellipses for Six Observers Who Completed the Full Set of 10 Chromaticities[a]

	Diameter 32 min			Diameter 48 min			Diameter 2.4°		
Ellipse	**L1**	**L2**	***θ***	**L1**	**L2**	***θ***	**L1**	**L2**	***θ***
1. D65 (0.6552)	0.00768	0.002632	101.5	0.003221	0.001488	105.3	0.00076	0.000523	147.5
2. Vert (0.018)	0.008262	0.002653	100.2	0.00334	0.001588	98.0	0.000713	0.000704	74.3
3. Vert (0.1)	0.017378	0.003492	101.6	0.016157	0.002647	99.6	0.00980	0.001444	91.0
4. Horiz (0.62)	0.008074	0.004765	83.7	0.004066	0.003313	57.2	0.002114	0.000718	7.0
5. Horiz (0.75)	0.012644	0.006901	136.7	0.006769	0.003868	160.5	0.003013	0.000994	1.8
6. 135° (0.6)	0.014595	0.005536	108.9	0.01030	0.003268	110.1	0.005242	0.001571	111.8
7. 135° (0.667)	0.005711	0.002687	106.0	0.002996	0.001695	113.3	0.000941	0.000606	146.7
8. 45° (0.68)	0.011102	0.003762	105.3	0.005844	0.002610	97.3	0.002358	0.001377	72.7
9. 165° (0.62)	0.006903	0.004755	100.76	0.003456	0.002932	145.2	0.0018274	0.000785	159.8
10. 165° (0.67)	0.006126	0.002686	108.5	0.002873	0.0018	124.75	0.001049	0.000422	173.1

[a]The leftmost columns give the number of the referent chromaticity and the L/(L + M) coordinate of the referent chromaticity [for the two referents placed on the vertical line (ellipses 2 and 3), the values are S/(L + M)]. For each ellipse, the lengths of the two axes (L1 and L2) and the orientation of the longer axis from the right horizontal (θ) are given.

This first principle has its antecedent in Judd's "superimportance of hue differences": Suprathreshold color differences estimated along a line of increasing colorimetric purity are smaller than would be predicted from the hue differences measured in an orthogonal direction at the same point in the color space [34]. When the referent chromaticities lie on the vertical or horizontal lines in the MacLeod–Boynton diagram (Figs. 3 and 4) and when—according to classical theory—the hue and saturation thresholds depend on independent chromatic signals, it is straightforward to explain the higher thresholds for saturation: the hue threshold, in such cases, depends on a channel that is near its equilibrium point (as set by the neutral-adapting field), whereas the purity (saturation) threshold depends on a channel that is polarized. In other cases, where hue and saturation thresholds each depend on both the classical channels, we have suggested that correlated noise could account for the elevation of saturation thresholds [15]. However, this explanation does not account for our finding that, when full ellipses are measured, the ellipse is not perfectly aligned with the line of increasing purity but is often rotated in a tritan direction (e.g., Fig. 5), and we consider an alternative hypothesis below.

(ii) For small targets, almost all ellipses are aligned approximately vertically in the MacLeod–Boynton diagram, i.e., in the tritan direction: discrimination is poorest when it depends on the short-wave cones alone.

Although all thresholds increase as the target size is reduced, this is especially true for discriminations in the tritan direction. "Foveal tritanopia" and "small-field tritanopia" have long been recognized properties of human vision (e.g., [35–37]). A clear explanation is found in the sparsity of short-wave cones throughout the retina and in the complete absence of such receptors in the very center of the fovea [23]. "Foveal tritanopia" is a misleading term, since the area from which short-wave cones are excluded is much smaller than the fovea, or indeed the

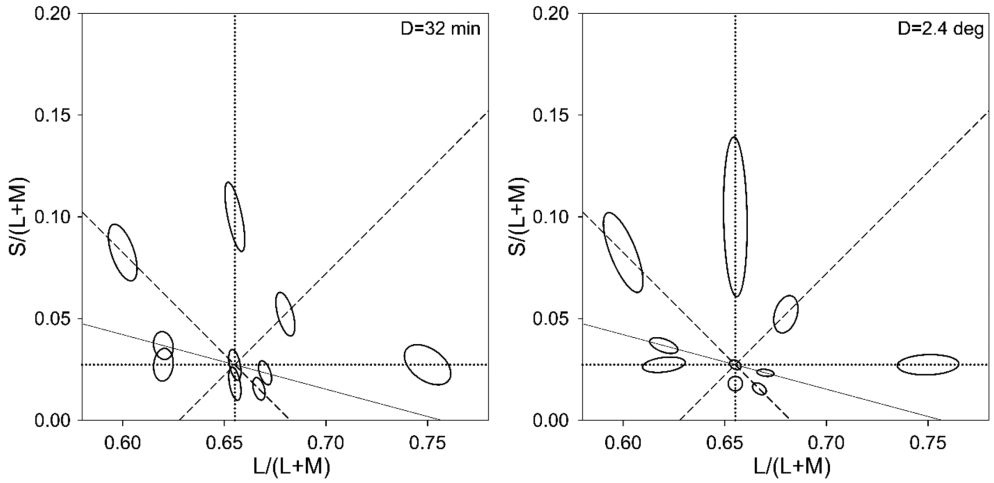

Fig. 8. Fitted ellipses are plotted for the largest and for the smallest sizes of the test. Left panel (32 min targets): the true ellipses are plotted for the smallest size. Right panel (2.4° targets): the ellipses are magnified four times compared to the actual measurements.

foveola, and typically corresponds to a visual angle of ∼20 min [38,39]; but this region must be a major factor in the elevated tritan thresholds for our smallest targets, which were of 32 angular minutes and were centrally fixated.

B. Possible Role of Non-Cardinal Chromatic Channels

One set of discrimination thresholds were measured around the adapting chromaticity, which was a metamer of D65. The MacLeod–Boynton diagram was scaled so that the line connecting unique blue and unique yellow was at the angle 135°. Our procedure did not allow the measurement of purity discrimination thresholds at D65, as in each direction, we used targets and distractors on opposite sides of the referent, and thus our observers always performed a hue discrimination.

If discrimination depended on two independent cardinal chromatic channels, corresponding to the axes of the MacLeod–Boynton chromaticity diagram, then we might expect the data points to be described by only one of three forms: a vertical ellipse, a horizontal ellipse, or a circle. In fact, the empirical results for the largest field (Fig. 2, 2.4°) are fitted by an ellipse with a negative tilt. The orientation is not exactly 135°; it is 147.5° (150° for the larger group of observers, see Supplement 1), but of course, the exact orientation depends on the arbitrary scaling of the ordinate of the diagram.

Discrimination ellipses of negative slope at the white point have often been reported previously [31,33,40–44], although not always [8]. One possible explanation for the negative slope is that the early visual system contains a channel that draws synergistic inputs from long- and short-wave cones and a signal of opposite sign from middle-wave cones. Such a channel has previously been postulated on the basis of psychophysical results (e.g., [8,22,45]), and in classical electrophysiological literature, there are occasional reports of cells with the required properties (e.g., [46,47]). The existence of such cells has been rendered plausible by recent connectomic work on the human fovea, suggesting that large bistratified ganglion cells and inner midget ganglion cells could receive the appropriate input connections [48,49] and by measurements of the light responses of individual ganglion cells of the macaque eye *in vivo*, using calcium imagining and adaptive optics [50].

An (L + S) versus M channel would explain the form of the central ellipse at D65. It would also explain our earlier finding of a locus of minimal thresholds that runs with a negative slope, close to the locus of unique blues [22,45]. Krauskopf and Gegenfurtner [8] postulated such a channel to explain the negative tilt of their discrimination ellipse in the upper left quadrant of their color space. Yet, why are our ellipses in this region [Fig. 5(a)] tilted clockwise from the 135° line along which only colorimetric purity varies? One interesting possibility is that the short-wave cone contribution to an (L + S) versus M channel is compressive in this region, making smaller and smaller contributions to the combined L + S signal.

There have also been recurrent suggestions of an (M + S) versus L retinal channel [46,47,50]. It is possible that a channel of this type accounts for the form of the large-field ellipse that lies on the 45° line (Fig. 6). It would be again necessary to postulate that the contribution of the S-cone signal is attenuated when the absolute S-cone signal is high.

C. Why Are the Ellipses Rotated from the Tritan Line for Very Small Fields?

The ellipse shown for the largest field at a chromaticity on the tritan line above D65 is perfectly aligned with the tritan axis [Fig. 3(b)]. This result gives confidence that our average observer corresponds to the DeMarco–Pokorny–Smith observer [21] and that our calibrations are correct. We might traditionally suppose that the L versus M channel is in equilibrium, while the S versus (L + M) channel is driven into a saturating region of its response function.

However, as the field size is reduced, the ellipse shows a small but clear anti-clockwise rotation from the tritan line. To understand why this might be, we must acknowledge that the DeMarco–Pokorny–Smith fundamentals, from which our

MacLeod–Boynton diagram is constructed, are those of a 2° observer. The spectral sensitivities of the cones (estimated at the cornea) will change when the targets become smaller. First, the density of the macular pigment will be higher [51–54]. Second, owing to the increased length of cones in the foveolar bundle, the optical density of the cones will increase [55], and in consequence, the absorption spectra of the cones will be broadened [56,57]. The relative effects of these factors could be examined analytically by varying the retinal position that is probed or by making independent psychophysical estimates of the macular pigment density and the cone optical density in individual observers.

For the present, as an illustration, we model how an increase in macular pigment would alter the orientation of those ellipses on the tritan line through D65 that corresponds to targets of 32 min [see, e.g., Figs. 2, 3(a), and 3(b)]. In each case, we take our empirically recorded RGB values for the individual threshold points and replot them for the same DeMarco–Pokorny–Smith 2° observer, assuming that the observer is viewing the physical stimuli through an additional filter, with the absorbance spectrum of macular pigment, and assuming no change in the optical density of the cones themselves. Our modeling suggests that a 60% increase in the macular pigment would yield an ellipse that is oriented vertically, i.e., along a tritan line. In each panel of Fig. 9, the left-hand ellipse is replotted from our earlier figures, and the right-hand ellipse shows where the data points would plot for the same DeMarco–Smith–Pokorny observer, if that observer was viewing through a 60% additional density of the macular pigment. Intermediate additions of the macular pigment give intermediate tilts.

Why does the macular pigment change the orientations of the ellipses, and why do the ellipses move downward and rightward in the MacLeod–Boynton chromaticity diagram? The macular pigment maximally absorbs light in the region of 460 nm. To explain the downward shift of the modeled ellipses seems straightforward: the additional macular pigment must necessarily attenuate the excitation of the short-wave cones and so shift the stimuli downward along the y axis, which represents S/(L + M). However, it is also the case that the ratio of sensitivity of middle-wave to long-wave cones is maximal close to 460 nm for the DeMarco–Pokorny–Smith observer. This is required by tritanopic color–matching functions [35,58,59]. The higher the S/(L + M) coordinate of our stimuli, the more power is in the 460 nm region of the broadband stimuli emitted by the CRT. Increasing the density of the macular pigment will thus disproportionately attenuate the excitation of middle-wave cones, and so increase the L/(L + M) coordinates of our stimuli. This will rotate each ellipse clockwise and will shift it bodily rightward.

We can also ask what would be the effect of such an additional macular pigment on the ellipse along the 135° line in the upper left-hand quadrant of the MacLeod–Boynton diagram. This ellipse, like that for large targets, has an orientation intermediate between a tritan (vertical) line and a line of increasing colorimetric purity [Fig. 5(a)]. Interestingly, the ellipse for small targets rotates only slightly when a 60% increase in the macular pigment is modeled, although it does move downward and rightward, as expected from the reasoning above. This is shown in Fig. 10, where we also plot the transformation that would be expected for the corresponding ellipse along the 135° line in the bottom right quadrant of the MacLeod–Boynton diagram.

This strictly illustrative modeling shows how variation in the optical density of the macular pigment might alter the discrimination ellipses for small, foveolar targets. The increase in density required by our modeling is compatible with several psychophysical estimates of the spatial profile of the macular pigment (e.g., [60,61]). However, further understanding will require analytical experiments and a consideration of variations in the optical density of the cones themselves.

Funding. Biotechnology and Biological Sciences Research Council (Grant BB/S000623/1).

Acknowledgment. M. V. D. was supported by a research project at the Kharkevitch Institute (Moscow). We are grateful to Professor John Barbur for the discussion of the effects of macular pigment, to the colleagues and students

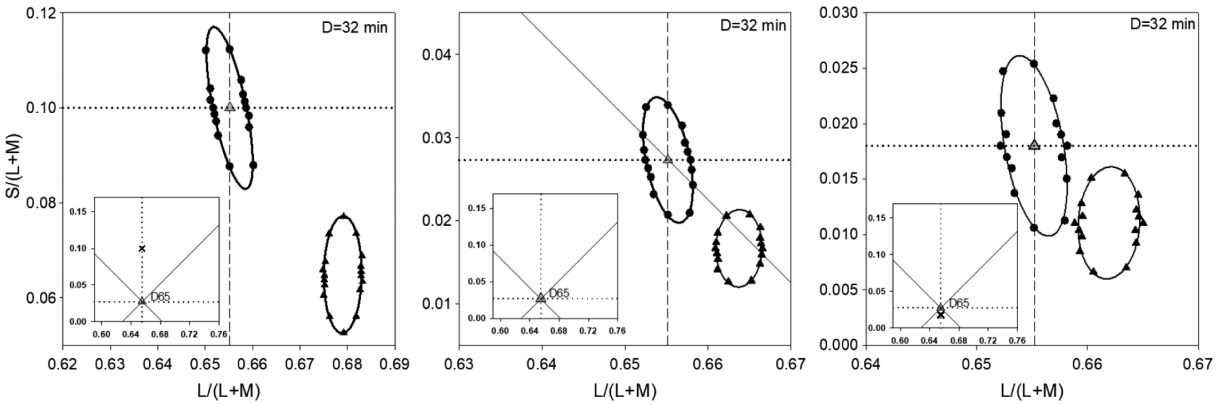

Fig. 9. Modeling of the effects of an increased macular pigment in the center of the foveola. The three panels show the results for the three referent points on the tritan line that runs vertically through the neutral point (metameric to D65). The leftmost panel corresponds to the referent below D65 [Fig. 3(a)], the central panel to D65 itself (Fig. 2), and the rightmost panel to the referent above D65 [Fig. 3(b)]. In each case, the large gray triangle shows the location of the referent chromaticity, and the solid circular data points show the empirical data for the smallest target size. The right-hand ellipse and the solid triangles in each panel show how the data would plot for the same DeMarco–Pokorny–Smith observer after a 60% increase in the macular pigment.

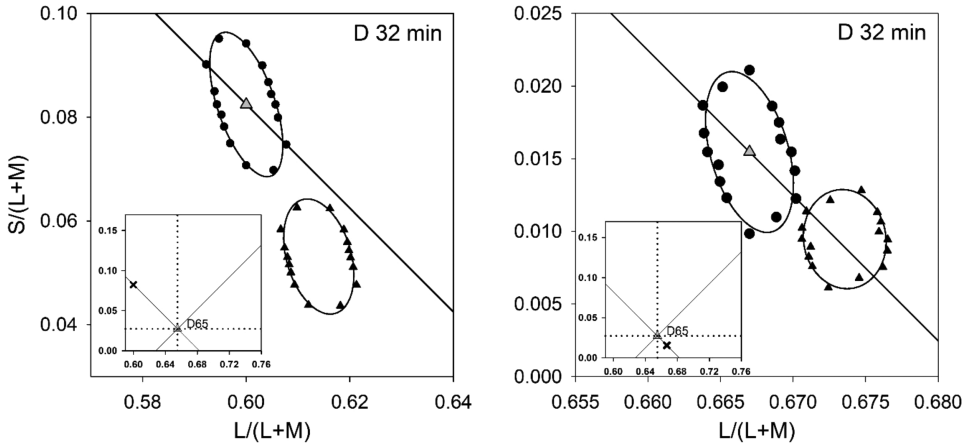

Fig. 10. Modeling the effect of increased macular pigment for the two referents placed on the 135° line—to the left, the referent in the upper left quadrant of the chromaticity diagram, and to the right, the referent in the lower right quadrant. In each panel, the large gray triangle shows the location of the referent and the circular solid points show the original data (replotted from Fig. 5). The right-hand ellipse in each panel and the solid triangles show how the data would plot for the same DeMarco–Pokorny–Smith 2° observer with a 60% increase in the macular pigment.

who served as observers, and to Jintong Hu and Lynne Ling for assistance with the fitting of ellipses.

Disclosures. The authors declare no conflicts of interest.

Data availability. Data underlying the results presented in this paper are not publicly available at this time but may be obtained from the authors upon reasonable request.

Supplemental document. See Supplement 1 for supporting content.

REFERENCES

1. K. J. McCree, "Small-field tritanopia and the effects of voluntary fixation," Opt. Acta **7**, 317–323 (1960).
2. W. R. J. Brown, "The effect of field size and chromatic surroundings on color discrimination," J. Opt. Soc. Am. **42**, 837–844 (1952).
3. D. L. MacAdam, "Small-field chromaticity discrimination," J. Opt. Soc. Am. **49**, 1143–1146 (1959).
4. G. T. Yonemura and M. Kasuya, "Color discrimination under reduced angular subtense and luminance," J. Opt. Soc. Am. **59**, 131–135 (1969).
5. N. V. Lobanova and G. N. Rautian, "Bolshie polya v kolorimeyrii (Large fields in colorimetry)," Dokl. Academii Nauk SSSR **69**, 1025–1028 (1949).
6. K. J. W. Craik, "The effect of adaptation upon visual acuity," Brit. J. Psychol. **29**, 252–266 (1939).
7. J. M. Loomis and T. Berger, "Effects of chromatic adaptation on color discrimination and color appearance," Vis. Res. **19**, 891–901 (1979).
8. J. Krauskopf and K. Gegenfurtner, "Color discrimination and adaptation," Vis. Res. **32**, 2165–2175 (1992).
9. V. C. Smith, J. Pokorny, and H. Sun, "Chromatic contrast discrimination: data and prediction for stimuli varying in L and M cone excitation," Color Res. Appl. **25**, 105–115 (2000).
10. W. Schönfelder, "Der Einfluss des Umfeldes auf die Sicherheit der Einstellung von Farbengleichungen," Z. Sinnesphysiol. **63**, 228–251 (1933).
11. D. L. MacAdam, "Visual sensitivities to color differences in daylight," J. Opt. Soc. Am. **32**, 247–281 (1942).
12. J. Pokorny, "Review: Steady and pulsed pedestals, the how and why of post-receptoral pathway separation," J. Vis. **11**(5):7, 1–23 (2011).
13. D. I. A. MacLeod and R. M. Boynton, "Chromaticity diagram showing cone excitation by stimuli of equal luminance," J. Opt. Soc. Am. **69**, 1183–1185 (1979).
14. S. E. Regan, R. J. Lee, D. I. MacLeod, *et al.*, "Are hue and saturation carried in different neural channels?" J. Opt. Soc. Am. A **35**, B299–B308 (2018).
15. M. V. Danilova and J. D. Mollon, "Superior discrimination for hue than for saturation and an explanation in terms of correlated neural noise," Proc. Biol. Sci. **283**, 20160164 (2016).
16. D. B. Judd, "Hue saturation and lightness of surface colors with chromatic illumination," J. Res. Nat. Bur. Stand. **24**, 293–333 (1940).
17. C. Witzel, J. Maule, and A. Franklin, "Red, yellow, green, and blue are not particularly colorful," J. Vis. **19**(14), 27 (2019).
18. M. V. Danilova and J. D. Mollon, "Symmetries and asymmetries in chromatic discrimination," J. Opt. Soc. Am. A **31**, A247–A253 (2014).
19. R. T. Eskew, "The gap effect revisited: slow changes in chromatic sensitivity as affected by luminance and chromatic borders," Vis. Res. **29**, 717–729 (1989).
20. M. V. Danilova and J. D. Mollon, "The gap-effect is exaggerated in the parafovea," Visual Neurosci. **23**, 509–517 (2006).
21. P. J. DeMarco, J. Pokorny, and V. C. Smith, "Full-spectrum cone sensitivity functions for X-chromosome linked anomalous trichromats," J. Opt. Soc. Am. A **9**, 1465–1476 (1992).
22. M. V. Danilova and J. D. Mollon, "Foveal color perception: minimal thresholds at a boundary between perceptual categories," Vis. Res. **62**, 162–172 (2012).
23. C. A. Curcio, K. A. Allen, K. R. Sloan, *et al.*, "Distribution and morphology of human cone photoreceptors stained with anti-blue opsin," J. Comp. Neurol. **312**, 610–624 (1991).
24. R. G. Kuehni, "Variability in unique hue selection: a surprising phenomenon," ColorRes. Appl. **29**, 158–162 (2004).
25. G. Jordan and J. D. Mollon, "Unique hues in heterozygotes for protan and deutan deficiencies," in *Colour Vision Deficiencies*, C. R. Cavonius, ed. (Kluwer, 1997), pp. 67–76.
26. S. M. Wuerger, P. Atkinson, and S. J. Cropper, "The cone inputs to the unique-hue mechanism," Vis. Res. **45**, 3210–3223 (2005).
27. K. C. McDermott and M. A. Webster, "Uniform color spaces and natural image statistics," J. Opt. Soc. Am. A **29**, A182–A187 (2012).
28. G. B. Wetherill and H. Levitt, "Sequential estimation of points on a psychometric function," Br. J. Math. Statist. Psych. **18**, 1–10 (1965).
29. O. Estévez, H. Spekreijse, J. T. W. Van Dalen, *et al.*, "The Oscar color vision test: theory and evaluation (objective screening of color anomalies and reductions)," Am. J. Optom. Physiol. Opt. **60**, 892–901 (1983).
30. A. Fitzgibbon, M. Pilu, and R. B. Fisher, "Direct least square fitting of ellipses," IEEE Trans. Pattern Anal. Mach. Intell. **21**, 476–480 (1999).
31. R. M. Boynton, A. L. Nagy, and C. X. Olson, "A flaw in equations for predicting chromatic differences," Color Res. Appl. **8**, 69–74 (1983).

32. J. D. Mollon, "Monge: The Verriest Lecture, Lyon, July 2005," Visual Neurosci. **23**, 297–309 (2006).
33. J. M. Bosten, R. D. Beer, and D. I. A. MacLeod, "What is white?" J. Vis. **15**(16), 5 (2015).
34. D. B. Judd, "Ideal color space," Color Eng. **8**, 37–52 (1970).
35. E. N. Willmer and W. D. Wright, "Colour sensitivity of the fovea centralis," Nature **156**, 119–121 (1945).
36. E. N. Willmer, "Colour of small objects," Nature **153**, 774–775 (1944).
37. G. Wald, "Blue-blindness in the normal fovea," J. Opt. Soc. Am. **57**, 1289–1301 (1967).
38. D. R. Williams, D. I. A. Macleod, and M. M. Hayhoe, "Foveal tritanopia," Vis. Res. **21**, 1341–1356 (1981).
39. D. R. Williams, D. I. A. Macleod, and M. M. Hayhoe, "Punctate sensitivity of the blue-sensitive mechanism," Vis. Res. **21**, 1357–1375 (1981).
40. D. I. Bramwell and A. C. Hurlbert, "Measurements of colour constancy by using a forced-choice matching technique," Perception **25**, 229–241 (1996).
41. R. D. Beer, A. Dinca, and D. I. A. MacLeod, "Ideal white can be yellowish or bluish, but not reddish or greenish," J. Vis. **6**(6), 417 (2006).
42. B. Pearce, S. Crichton, M. Mackiewicz, *et al.*, "Chromatic illumination discrimination ability reveals that human colour constancy is optimised for blue daylight illuminations," Plos One **9**, e87989 (2014).
43. B. C. Regan and J. D. Mollon, "Discrimination ellipses in the MacLeod-Boynton diagram: results for normal and colour-deficient subjects obtained with a CRT display," in *Colour Vision Deficiencies XII*, B. Drum, ed. (1995), pp. 445–451.
44. T. Hansen, M. Giesel, and K. R. Gegenfurtner, "Chromatic discrimination of natural objects," J. Vis. **8**(1):2, 1–19 (2008).
45. M. V. Danilova and J. D. Mollon, "Parafoveal color discrimination: a chromaticity locus of enhanced discrimination," J. Vis. **10**(1):4, 1–9 (2010).
46. F. M. De Monasterio, P. Gouras, and D. J. Tolhurst, "Trichromatic colour opponency in ganglion cells of the rhesus monkey retina," J. Physiol. **251**, 197–216 (1975).
47. A. Valberg, B. B. Lee, and D. A. Tigwell, "Neurons with strong inhibitory S-cone inputs in the macaque lateral geniculate nucleus," Vis. Res. **26**, 1061–1064 (1986).
48. Y. J. Kim, O. Packer, A. Pollreisz, *et al.*, "Comparative connectomics reveals noncanonical wiring for color vision in human foveal retina," Proc. Natl. Acad. Sci. Am. USA **120**, 12 (2023).
49. Y. J. Kim, O. Packer, and D. M. Dacey, "A circuit motif for color in the human foveal retina," Proc. Natl. Acad. Sci. U.S.A. **121**, 1–11 (2024).
50. T. Godat, K. Kohout, K. Parkins, *et al.*, "Cone-opponent ganglion cells in the primate fovea tuned to noncardinal color directions," J. Neurosci. **44**, e1738232024 (2024).
51. D. M. Snodderly, J. D. Auran, and F. C. Delori, "The macular pigment. II. Spatial-distribution in primate retinas," Invest. Ophthalmol. Vis. Sci. **25**, 674–685 (1984).
52. D. M. Snodderly, P. K. Brown, F. C. Delori, *et al.*, "The macular pigment. I. Absorbance spectra, localization, and discrimination from other yellow pigments in primate retinas," Invest. Ophthalmol. Vis. Sci. **25**, 660–673 (1984).
53. S. F. Chen, Y. Chang, and J. C. Wu, "The spatial distribution of macular pigment in humans," Curr. Eye Res. **23**, 422–434 (2001).
54. P. E. Kilbride, K. R. Alexander, M. Fishman, *et al.*, "Human macular pigment assessed by imaging fundus reflectometry," Vis. Res. **29**, 663–674 (1989).
55. A. E. Elsner, S. A. Burns, and R. H. Webb, "Mapping cone photopigment optical density," J. Opt. Soc. Am. A **10**, 52–58 (1993).
56. P. B. M. Thomas, M. A. Formankiewicz, and J. D. Mollon, "The effect of photopigment optical density on the color vision of the anomalous trichromat," Vis. Res. **51**, 2224–2233 (2011).
57. J. Pokorny and V. C. Smith, "Effect of field size on red–green color mixture equations," J. Opt. Soc. Am. **66**, 705–708 (1976).
58. W. D. Wright, "The characteristics of tritanopia," J. Opt. Soc. Am. **42**, 509–521 (1952).
59. J. D. Mollon, O. Estévez, and C. R. Cavonius, "The two subsystems of colour vision and their roles in wavelength discrimination," in *Vision: Coding and Efficiency*, C. Blakemore, ed. (Cambridge University, 1990), pp. 119–131.
60. J. S. Werner, S. K. Donnelly, and R. Kliegl, "Aging and human macular pigment density—appended with translations from the work of Schultze, Max and Hering, Ewald," Vis. Res. **27**, 257–268 (1987).
61. J. L. Barbur, E. Konstantakopoulou, M. Rodriguez-Carmona, *et al.*, "The Macular Assessment Profile test—a new VDU-based technique for measuring the spatial distribution of the macular pigment, lens density and rapid flicker sensitivity," Ophthal. Physiol. Opt. **30**, 470–483 (2010).